CHAPTER III

RESULTS AND DISCUSSION

Syntheses of aminoethylprolyl (*aep*) PNA have been previously reported, however, the methods were complicated and provided only moderate yield. Kumar [45] and Lui [47] have reported that *N*-alkylation of *trans*-4-hydroxy-L-proline methyl ester with *N*-Boc-aminoethylbromide to afford the *cis*-(*N*-Boc-aminoethyl)-L-proline methyl ester in 60 and 68 % respectively. The report of Vilaivan described the nucleophilic ring opening of the *N*-Nosylazilidine by a *C*-protected of *cis*-4-T^{Bz}-D-proline diphenylmethyl ester followed by protecting group conversion to Fmoc group gave the *N*-protected of *cis*-(*N*-Fmoc-aminoethyl)-4-T^{Bz}-D-proline diphenylmethyl ester in 22 % yield (5 step) [48]. In order to improve the efficiency in *aep*PNA syntheses, the coupling step between proline derivative and the ethylene spacer has to be improved.

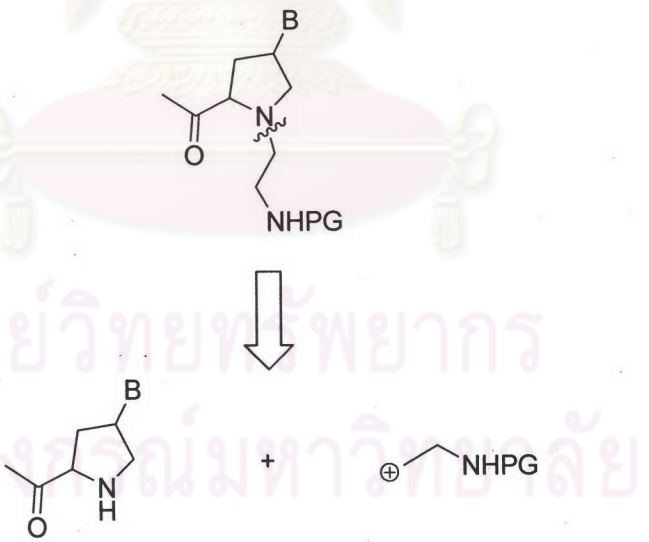

Figure 3.1 Retrosynthetic analyses for synthesis of *aep*PNA

According to retrosynthetic analysis (**Figure 3.1**), three most important routes might be feasible which includes i) nucleophilic substitution of a suitably protected aminoethyl synthon such as *N*-protected aminoethyl halide by a proline derivative ii) nucleophilic addition to activated aziridine by a proline derivative iii) reductive

alkylation of a proline derivative carrying free amino terminus by an aminoaldehyde according to **Figure 3.2**

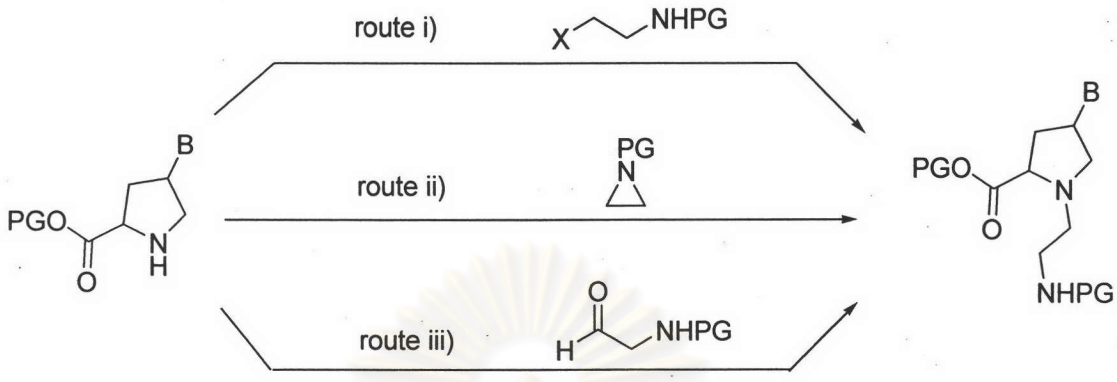

Figure 3.2 Possible routes to develop the synthesis of *aep*PNA

3.1 Synthesis of *aep*PNA

3.1.1 Synthesis of *aep*PNA by nucleophilic substitution of aminoethyl halide

This route has been previously reported by Kumar who described *N*-alklylation of the pyrrolidine ring in *trans*-4-hydroxy-L-proline methyl ester by *N*-Boc-aminoethyl bromide [45]. We initially followed this route due to the reported simplicity and availability of the starting materials. However, we chose to react the protected bromoethylamine derivative with nucleobase-modified proline instead of hydroxyproline as described by Kumar to make the synthesis more convergent. In order to do this, the amino group of bromoethylamine (**11**) must be protected with a temporary protecting group in order to avoid the undesired intramolecular nucleophilic displacement of the bromine by the nitrogen of the bromoethylamine. Two most popular urethane-type protecting group, namely *tert*-butoxycarbonyl (Boc) and fluoren-9-ylmethoxycarbonyl (Fmoc) were considered for this purpose. Boc protection has considerable advantages because it is inexpensive and remarkably stable towards both nucleophiles and bases which are expected to be the condition of nucleophilic substitution in the next steps. The Fmoc group is too base-labile, but it is the most desirable protecting group for SPPS. As a result, the Boc group was chosen as a temporary protecting group for the alkylation step then is will be exchanged with Fmoc for SPPS. Reaction between bromoethylamine (**11**) and di-*tert*-butyl

dicarbonate (Boc_2O) under base conditions gave *N-tert*-butoxycarbonyl-bromoethyl amine (**12**) and carbon dioxide as a by-product (**Figure 3.3**). The reaction mixture was worked up by acidification followed by extraction and evaporation to afford *N-tert*-butoxycarbonyl-bromoethylamine (**12**) (77 % yield). ^1H NMR analysis showed a characteristic singlet at 1.48 ppm with integration of 9H due to the Boc group and ^{13}C NMR showed signals at 28.3, 79.7 and 156.7 ppm of Boc $\underline{C}H_3$, Boc $\underline{C}$ and Boc $\underline{C}O$ respectively.

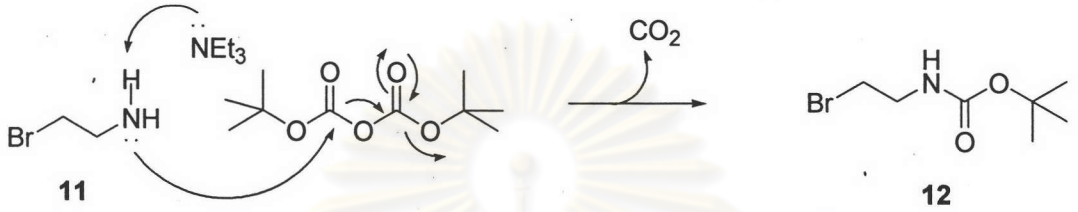

Figure 3.3 Reaction mechanism for synthesis of *N-tert*-butoxycarbonyl-bromoethyl amine (**12**)

Nucleophilic substitution of *N-tert*-butoxycarbonyl-bromoethylamine (**12**) with the intermediate (**6b**) after removal of the Boc group by treatment with *p*-toluenesulfonic acid/acetonitrile was carried out according to the procedure described by Vilaivan [38] for a similar reaction. Unfortunately, the desired product (**22**) was not obtained (**Figure 3.4**)

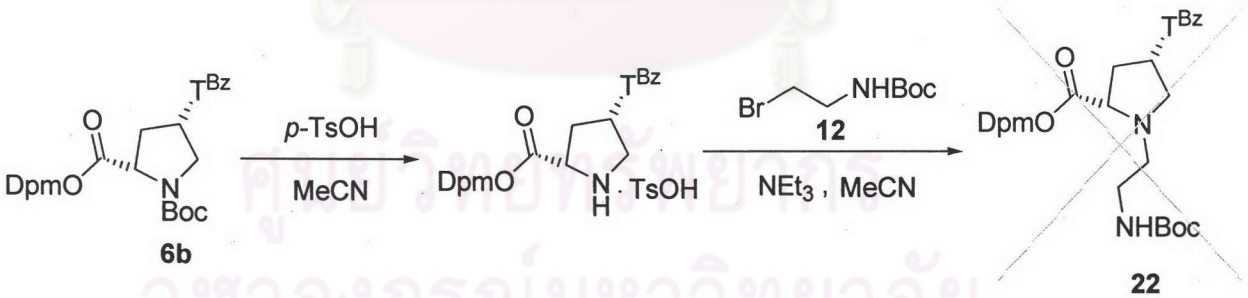

Figure 3.4 Synthesis of *N*-2-(*N*-Boc-amino)ethyl-*cis*-4-(N^3-benzoylthymin-1-yl)-L-proline diphenylmethyl ester (**22**) by nucleophilic substitution

It is possible that the secondary amino group in proline was probably not sufficiently nucleophilic to attack this relatively unreactive alkylating agent. Furthermore the bromoehtylamine derivative may also prone to intramolecular reactions such as formation of aziridine or oxazolidinone in the presence of a base.

According to Kumar's work [45], the *N*-alkylation of the pyrrolidine ring in *trans*-4-hydroxy-L-proline methyl ester by *N*-Boc-aminoethyl bromide afforded the 1-(*N*-Boc-aminoethyl)proline derivative, which is the analogue of desired compound. It was decided to follow this route; namely alkylation of *cis*-4-hydroxy-D-proline methyl ester (**10**) by Boc-bromoethylamine.

To obtain *cis*-4-hydroxy-D-proline methyl ester (**10**), *cis*-4-hydroxy-D-proline (**1b**) was refluxed in acetyl chloride and methanol mixture (**Figture 3.5**). ^{1}H NMR spectrum of product showed a characteristic singlet 3.72 ppm with integration of 3H due to the ester O$\underline{CH_3}$.

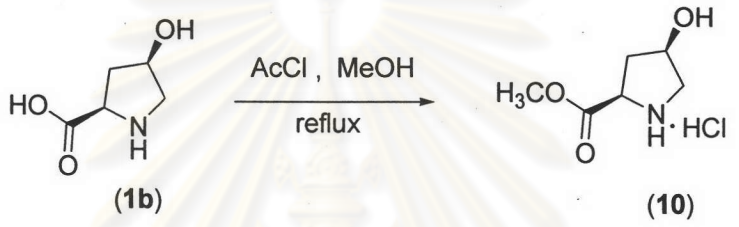

Figure 3.5 Synthesis of *cis*-4-hydroxy-D-proline methyl ester (**10**)

The next step was *N*-alkylation of *cis*-4-hydroxy-D-proline methyl ester (**10**) with Boc-bromoethylamine (**12**) under basic condition (**Figure 3.6**). The reaction mixture was worked up by acid-base extraction providing in 58 % yield of (**20**) as colorless oil. ^{1}H NMR spectrum of the product showed the important signal at 2.68-2.81 and 3.07-3.30 ppm which confirmed the presence of N-CH_2-CH_2-N moiety and a singlet peak at 1.47 ppm which indicated the presence of a Boc group (BocNHC$\underline{H_2}$C$\underline{H_2}$N).

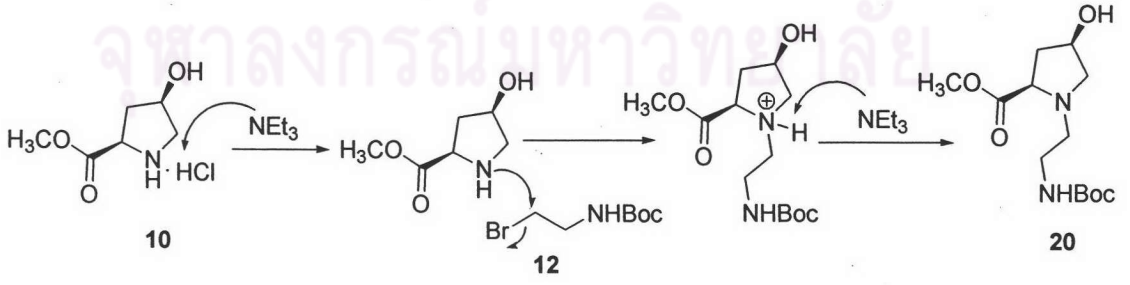

Figure 3.6 Reaction mechanism for synthesis of *N*-2-(*N*-Boc-amino)ethyl-*cis*-4-hydroxy-D-proline methyl ester (**20**)

The moderate yield is probably a consequence of formation of 2-oxazolidone as shown in **Figure 3.7**

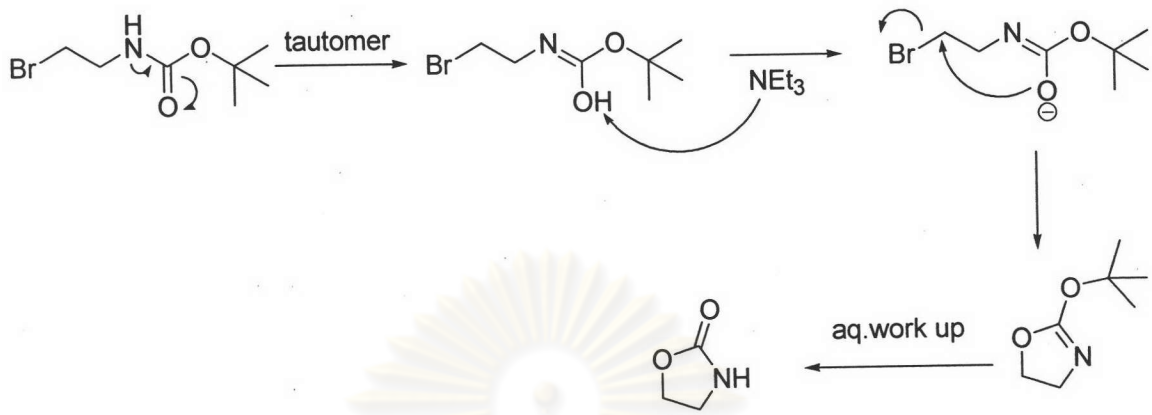

Figure 3.7 Possible mechanism of 2-oxazolidone formation

With our requirement that after the nucleobase alkylation, the product would have to retain the *cis*-D-configuration. Thus, the proline derivative must be converted into *trans*-D-isomer (first inversion) before alkylation with nucleobase (second inversion). Disappointingly, Mitsunobu reaction with formic acid as nucleophile did not provide the desired product (**21**) (**Figure 3.8**). This was confirmed by the absence of the signal of the aldehyde proton in the ^{1}H-NMR spectrum.

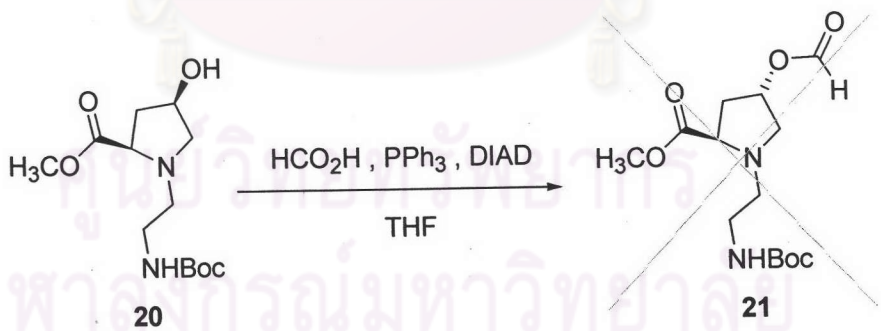

Figure 3.8 Inversion of configuration compound (**20**) by Mitsunobu reaction

Alternatively, *trans*-D-isomer (**10a**) was used as starting material. This was prepared by inverting the configuration of the *cis*-D-isomer (**10**a) by Mitsunobu reaction with formic acid followed by treatment with methanolic ammonia. It was then *N*-protected followed by coupling with Boc-bromoethylamine (**12**) to expect product (**10a**). After *N*-alklylation of *N*-Boc-aminoethyl bromide, incorporation of

thymine into the proline ring by Mitsinobu reaction gave the desired product (**Figure 3.9**). However, the replacement of the C-4 hydroxy function with T^{Bz} under Mitsunobu reaction condition as previously reported [38] provided the product in low yield (31 %). We therefore concluded that the method was not quite efficient and determined to find a new method for synthesis of the desired product.

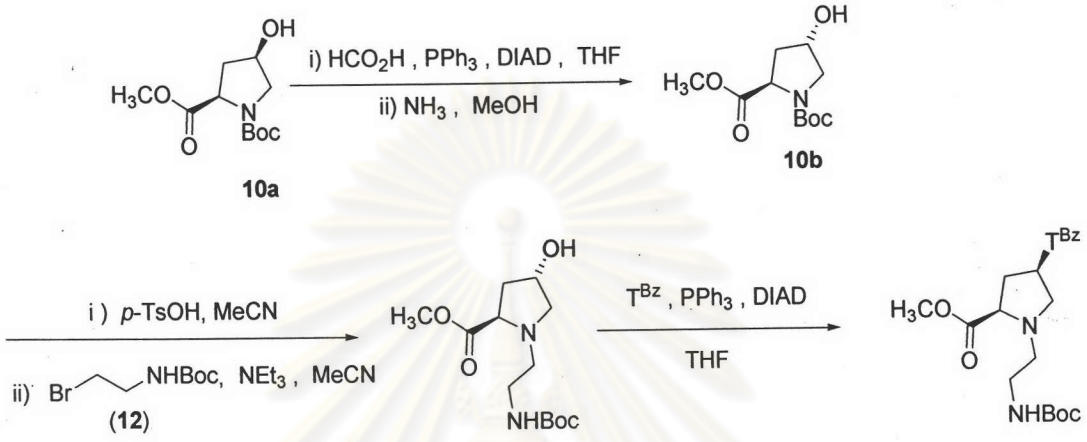

Figure 3.9 Pathway for synthesis of (2*R*,4*R*)-4-(N^3-benzoylthymin-1-yl) proline methyl ester

3.1.2 Synthesis of *aep*PNA by nucleophilic addition of activated aziridine

As mentioned above, nucleophilic substitution of protected aminoethyl bromide with proline derivative did not offer satisfactory results. An alternative idea was to employ aziridine ring opening reaction since aziridine may be considered as a highly reactive synthetic equivalent of aminoethyl group due to its high strain energy. Ring opening of aziridine requires activation of the nitrogen atom by electron withdrawing substituent such as *N*-acyl or *N*-sulfonyl group in order to enhance leaving ability of the nitrogen atom, and to prevent polymerization by the liberated nucleophilic free amino group. In 2000, the nucleophilic ring opening of the *N*-nosyl (Ns) aziridine by a nucleobase-modified proline derivative to afford the 1-(*N*-Ns-aminoethyl)proline derivative has been reported by Vilaivan *et. al.* [47]. However, synthesis of Ns-aziridine and subsequent manipulation of the nosyl protecting group to Fmoc group requires several and complicated steps. Improvement by using an easily removable protecting group such as Boc is therefore highly disirable.

N-tert-butoxycarbonylaziridine (**14**), an easy-synthesized activated aziridine, was synthesized from bromoethylamine·HCl (**11**) by treatment of the amine salt aqueous sodium hydroxide for 4 h followed by adding Boc_2O (**Figure 3.10**). ^1H NMR of this product revealed a singlet peak at 1.49 ppm with integration of 9H due to the Boc group and 2.17 ppm of symmetric aziridine aliphatic proton (2 x $C\underline{H}_2$). In addition, ^{13}C NMR spectrum revealed signals at 27.9 ppm of aziridine $\underline{C}H_2$ and, 28.3, 79.7 and 156.7 ppm of Boc $\underline{C}H_3$, Boc $\underline{C}$ and Boc $\underline{C}O$ respectively.

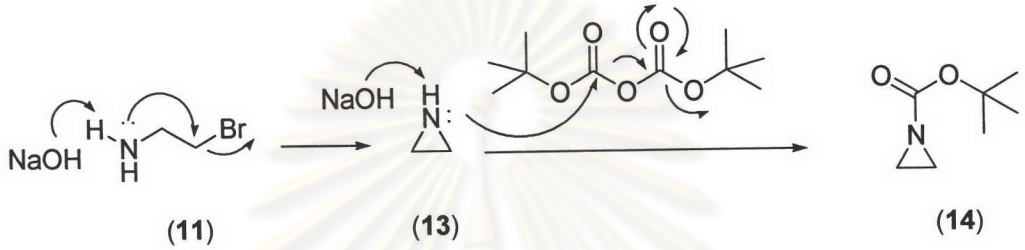

Figure 3.10 Reaction mechanism for synthesis of *N*-Boc-aziridine(**14**)

The desired Boc-aziridine (**14**) was reacted with the intermediate (**6b**) afer removal of the Boc group by treatment with *p*-toluenesulfonic acid/acetonitrile under basic conditions. Unfortunately, TLC analysis revealed that reaction did not provide the desired product (**Figure 3.11**) when compared with a reference standard [47]. It is possible that the Boc-aziridine was probably not sufficiently activated due to the relatively poor electron withdrawing effect of the Boc group there by making it a relatively unreactive alkylating agent.

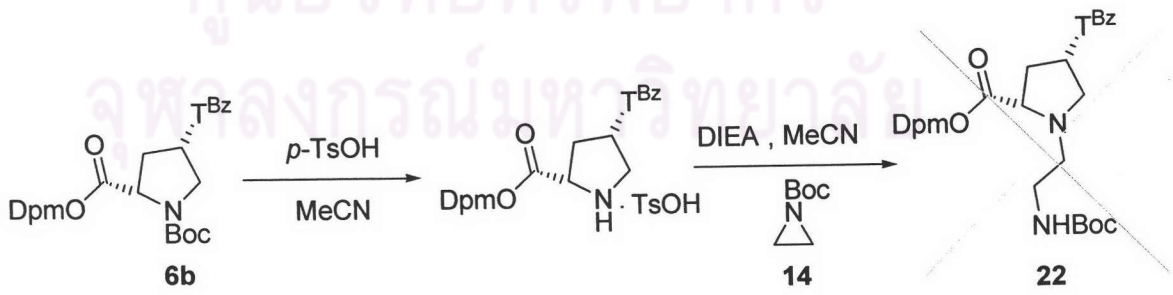

Figure 3.11 Synthesis of *N*-2-(*N*-Boc-amino)ethyl-*cis*-4-(N^3-benzoylthymin-1-yl)-L-proline diphenylmethyl ester (**22**) by nucleophilic ring opening of Boc-aziridine

3.1.3 Synthesis of *aep*PNA by reductive alkylation of aminoaldehyde

The alternative idea was to employ *N*-protected aminoaldehyde by reactive alkylation using *N*-Fmoc-aminoaldehyde to provide the Fmoc derivatives directly without the need for protecting group conversion. Brown has reported that a reductive alkylation of glycine derivative carrying free amino terminus with Boc-aminoaldehyde by $NaBH_3CN$ afforded the aminoethyl glycine derivative [51], which is structurally similar to our desired products. Boc-aminoaldehyde was therefore prepared following the procedure described [51]. Gratifyingly the reductive alkylation of nucleobase-modified proline derivative (**6a**) (after removed of Boc group) with Boc-aminoaldehyde in the presence of $NaBH_3CN$ afforded the desired product in 30 % yield (**Figure 3.12**).

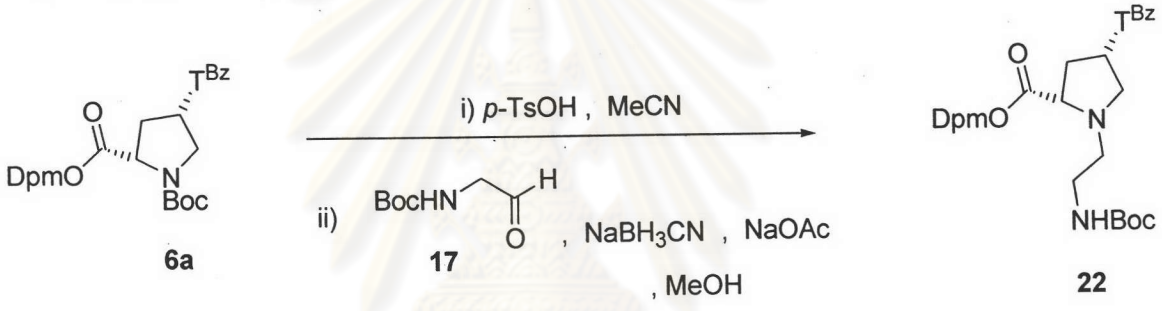

Figure 3.12 Synthesis of *N*-2-(*N*-Boc-amino)ethyl-*cis*-4-(N^3-benzoylthymin-1-yl)-L-proline diphenylmethyl ester (**22**) with Boc-aminoaldehyde

For solid phase peptide synthesis, it was considered that the Fmoc chemistry had a number of advantages over Boc chemistry. We therefore decided to attempt the direct reductive alkylation on using *N*-Fmoc-aminoaldehyde so that no further protecting group conversion is necessary.

3-amino-1,2-propanediol reacted with 9-fluoroenyl methyl chloroformate (FmocCl) under basic condition (**Figure 3.13**). The reaction mixture was worked up by acid-base extraction to afford a 90% yield of *N*-Fmoc-3-amino-1,2-propanediol (**18**) as a white solid. ^{1}H NMR spectrum show a characteristic signal at 4.24 and 4.50 ppm which belonged to Fmoc aliphatic C<u>H</u> and Fmoc aliphatic C<u>H</u>$_2$ respectively. In addition, Fmoc aromatic C<u>H</u> signals were found at 7.37-7.81 ppm. ^{13}C NMR spectrum revealed signals at 43.5 (Fmoc aliphatic <u>C</u>H), 70.9 (Fmoc aliphatic <u>C</u>H$_2$), 119.9-143.8 (Fmoc aromatic <u>C</u>H) and 157.2 (Fmoc <u>C</u>O) indicating successful protection.

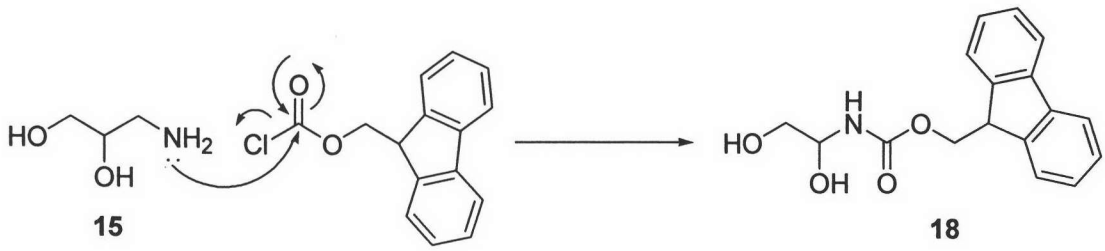

Figure 3.13 Reaction mechanism for synthesis of *N*-Fmoc-3-amino-1,2-propanediol (**18**)

N-Fmoc-aminoacetaldehyde (**19**) was prepared in 99% yield by oxidative cleavage of *N*-Fmoc-3-amino-1,2-propanediol (**18**) with $NaIO_4$ (**Figure 3.14**) following the procedure described for the corresponding Boc-aminoaldehyde [51]. ^1H NMR of product showed a characteristic signal at 9.17 ppm and ^{13}C NMR spectrum showed a signal at 196.6 ppm due to the aldehyde C<u>H</u>O.

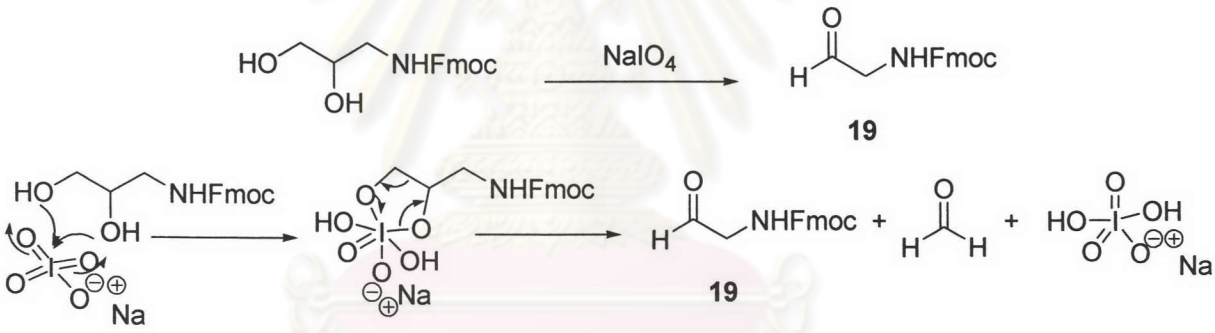

Figure 3.14 Reaction and mechanism for synthesis of *N*-Fmoc-aminoacetaldehyde (**19**)

Reductive alkylation of *N*-Fmoc-aminoacetaldehyde (**19**) with the intermediate (**6a**) after removal of the Boc group by treatment with *p*-toluenesulfonic acid/acetonitrile took place in the presence of $NaBH_3CN$/NaOAc. The role of NaOAc was probably to control the pH of the reaction to compromise between reactivity of $NaBH_3CN$ and stability of Fmoc. The reaction mixture was worked up by acid-base extraction and purified by column chromatography to give the desired product (**23**) as white foam in 76% yield (2 steps from **6a** and **19**) (**Figure 3.15**). ^1H NMR of the product showed the following important signals: 2.61-2.68 and 2.77-2.88 ppm (FmocNHCH$_2$C<u>H</u>$_2$N), 3.13-3.22 and 3.34-3.45 ppm (FmocNHC<u>H</u>$_2$CH$_2$N), 4.26 ppm

(Fmoc aliphatic C<u>H</u>), 4.36 and 4.52 ppm (Fmoc aliphatic C<u>H</u>$_2$) and 7.24-7.48, 7.82 and 7.92-8.00 (Fmoc aromatic C<u>H</u>), partially overlapped with some peaks of Dpm aromatic C<u>H</u> and benzoyl C<u>H</u>. In addition, ^{13}C NMR spectrum revealed signals of FmocNHCH$_2$<u>C</u>H$_2$N at 39.5 ppm, Fmoc NH<u>C</u>H$_2$CH$_2$N at 66.8 ppm, Fmoc aliphatic <u>C</u>H at 47.3 ppm, Fmoc aliphatic <u>C</u>H$_2$ at 65.0 ppm, Fmoc aromatic <u>C</u>H at 120.2, 125.3, 127.9 and 128.5 ppm and Fmoc aromatic <u>C</u> at 141.4, 144.0 and 144.0 ppm. The structure was further confirmed by comparison of NMR spectrum with the values reported in the literature [48].

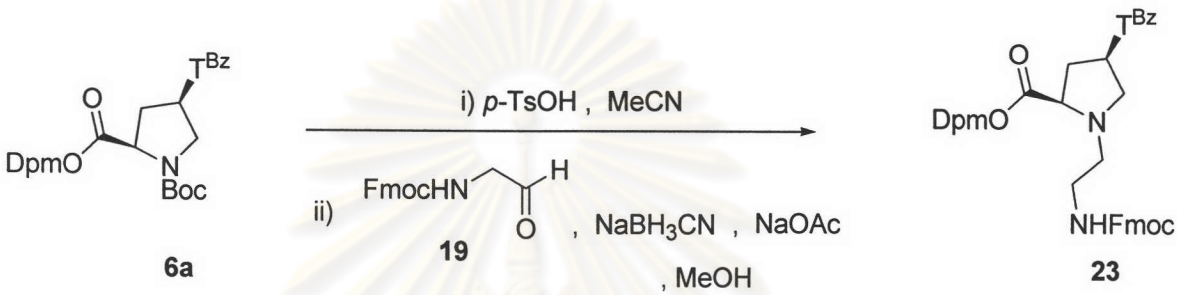

Figure 3.15 Synthesis of *N*-2-(*N*-Fmoc-amino)ethyl-*cis*-4-(N^3-benzoylthymin-1-yl)-D-proline diphenylmethyl ester (**23**) by reductive alkylation

After the coupling of *N*-Boc-*cis*-4-(N^3-benzoylthymin-1-yl)-D-proline diphenylmethyl ester (**6a**) with *N*-Fmoc-aminoacetaldehyde (**19**) by reductive alkylation was successful, other nucleobase-modified proline derivatives (*cis*-D-T^{Bz}, *trans*-D-T^{Bz}, *cis*-L-T^{Bz}, *trans*-L-T^{Bz}, *cis*-D-A^{Bz}, *cis*-D-C^{Bz}, *cis*-D-G^{Ibu}) were synthesized by the same method. The result was shown in **Table 3.1**.

Table 3.1 Synthesis of all intermediate proline derivatives by reductive alkylation with *N*-Fmoc-aminoaldehyde

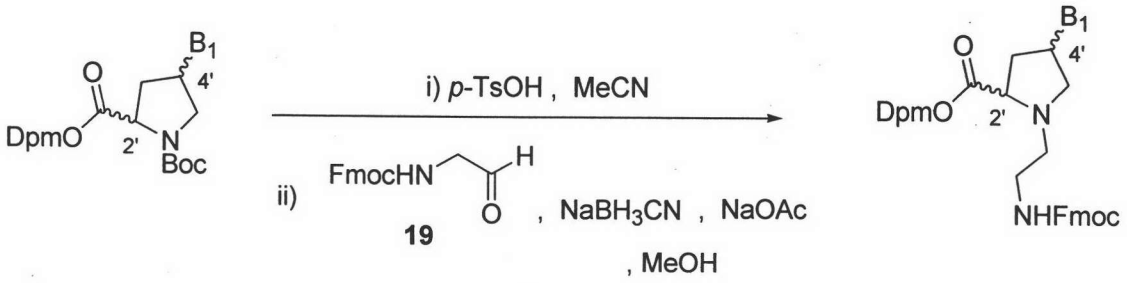

intermediate proline derive.	configuration at position 2' and 4' in proline ring	B_1	product	% yield
6a	(2*R*,4*R*)	T^{Bz}	**23**	76
6b	(2*S*,4*S*)	T^{Bz}	**24**	87
6c	(2*R*,4*S*)	T^{Bz}	**25**	40
6d	(2*S*,4*R*)	T^{Bz}	**26**	43
7	(2*R*,4*R*)	G^{Ibu}	**27**	69
8	(2*R*,4*R*)	A^{Bz}	**28**	60
9	(2*R*,4*R*)	C^{Bz}	**29**	89

Since the (2*S*,4*S*) product (**24**) is the opposite enantiomer of (2*R*,4*R*) product (**23**) therefore ^{1}H NMR and ^{13}C NMR spectrum of the two compounds were identical On the other hand, ^{1}H NMR spectra of (2*R*,4*S*) product (**25**) and (2*S*,4*R*) product (**26**), which is another enantiomer pairs showed the following important signal: 2.73 ppm (FmocNHCH$_2$C$\underline{H}_2$N), 3.30 ppm (FmocNHC$\underline{H}_2$CH$_2$N), 4.23 ppm (Fmoc aliphatic C$\underline{H}$), 4.28-4.45 ppm (Fmoc aliphatic C$\underline{H}_2$) and 7.27-7.49, 7.81 and 7.96 (Fmoc aromatic C$\underline{H}$), partially overlapped with some peaks of Dpm aromatic C$\underline{H}$. In addition, ^{13}C NMR spectra of the two compounds revealed signals of FmocNHCH$_2$C$\underline{H}_2$N at 39.34 ppm, Fmoc NHC$\underline{H}_2$CH$_2$N at 66.6 ppm, Fmoc aliphatic C$\underline{H}$ at 47.3 ppm, Fmoc aliphatic C$\underline{H}_2$ at 63.9 ppm, Fmoc aromatic C$\underline{H}$ at 120.1, 125.1, 127.8 and 128.3 ppm and Fmoc aromatic $\underline{C}$ at 141.3 and 143.9 ppm. The structure was further confirmed by ^{1}H-^{1}H COSY.

For compounds **27**, **28** and **29**, the NMR spectra showed characteristic patters due to proline, Fmoc and NHCH$_2$CH$_2$N similar to the corresponding to thymine compound (**23**). The product (**27**) also showed a characteristic signal of guanine at

8.14 ppm in ^{1}H NMR spectrum and 138.2, 147.9, 148.5, 156.0 ppm in ^{13}C NMR spectrum. The product (**28**) showed a characteristic signal of adenine at 8.65, 8.82 ppm in ^{1}H NMR spectrum and 133.8, 141.3, 149.4 151.5, 152.4 ppm in ^{13}C NMR spectrum. The product (**29**) showed a characteristic signal of cytosine at 8.43 ppm in ^{1}H NMR spectrum and 97.5, 146.8, 161.9 ppm in ^{13}C NMR spectrum.

The mechanism for this reductive alkylation step was demonstrated in **Figure 3.16**

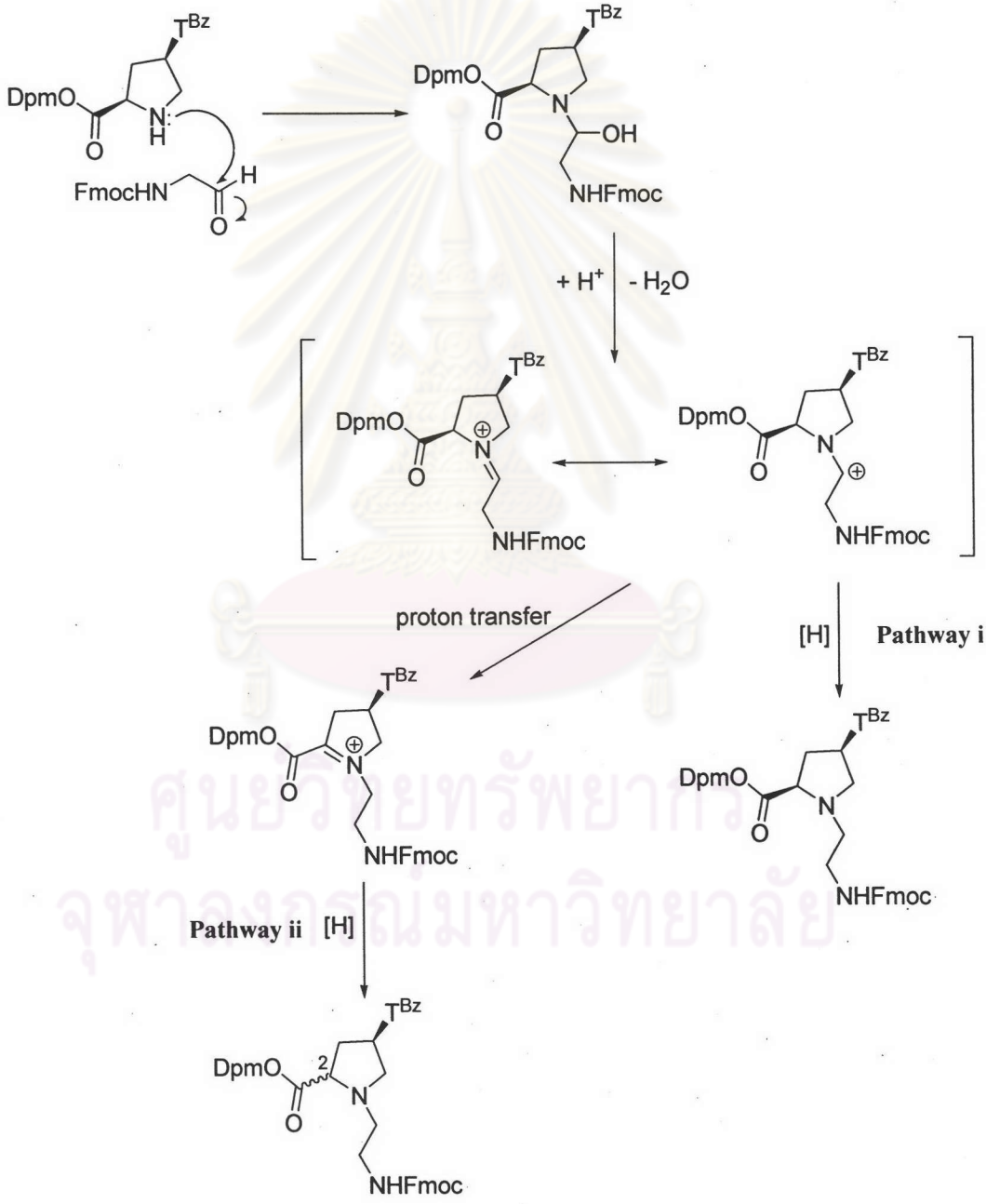

Figure 3.16 Coupling mechanism for synthesis of *N*-2-(*N*-Fmoc-amino)ethyl-*cis*-4-(N^3-benzoylthymin-1-yl)-D-proline diphenylmethyl ester (**23**)

According to the two possible mechanisms of reductive alkylation, the epimerization of the position 2′ in proline ring is possible *via* **Pathway ii** so mixture of *cis*-D (2*R*,4*R*) and *trans*-L (2*S*,4*R*) product may be obtained from this reaction. Since the *trans*-L (2*S*,4*R*) product which is diasteromer of *cis*-D (2*R*,4*R*) product showed distinctly different signals in ^{1}H NMR, the absence of the *trans*-L signal indicated that no epimerization had taken place(**Figure 3.17**). It can be concluded that the reaction precede mainly through **Pathway i** and therefore epimerization is not a problem for this reaction.

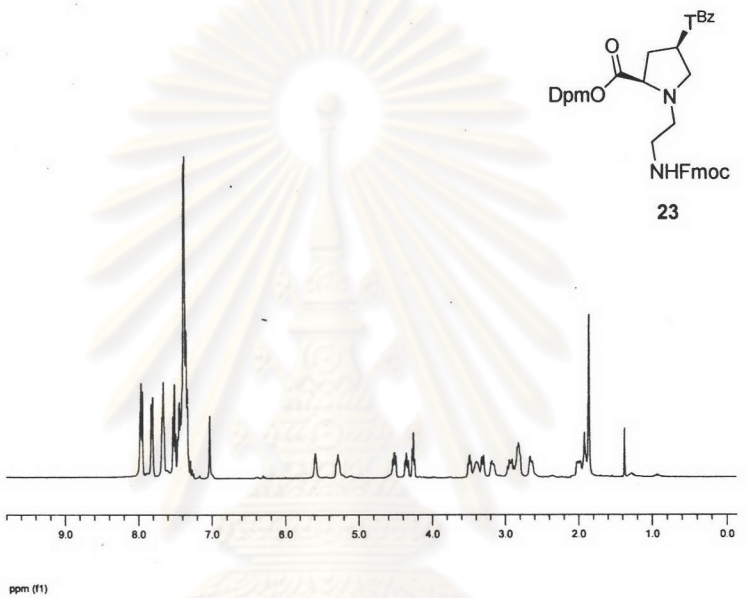

Figure 3.17 ^{1}H NMR Spectrum of CD-Fmoc-T^{Bz}-ODpm (**23**) synthesized from CD-proline derivative (**6a**)

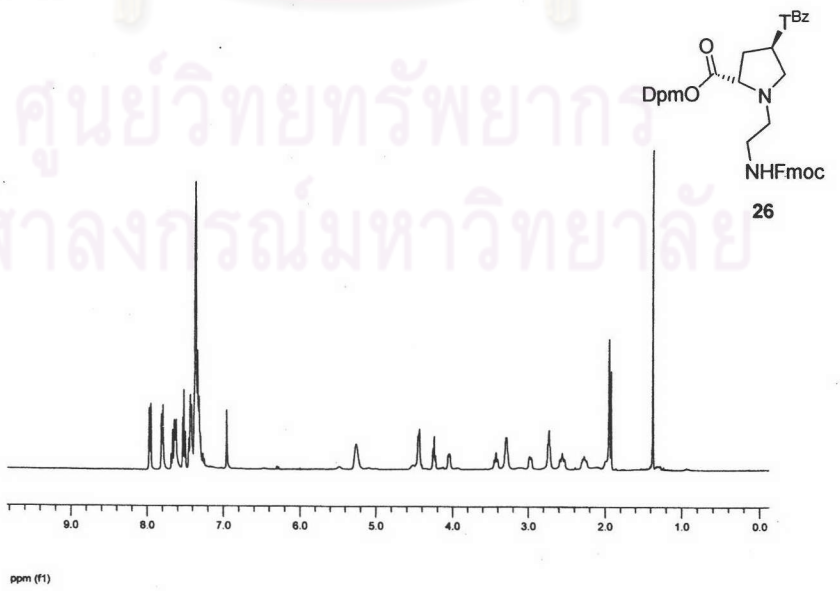

Figure 3.18 ^{1}H NMR Spectrum of TL-Fmoc-T^{Bz}-ODpm (**26**) synthesized from TL-proline derivative (**6d**)

Reductive alkylation of D-proline derivative containing nucleobase was a more efficient route for synthesis of PNA monomers than the previously reported methods. It provided the Fmoc derivatives directly without the need for protecting group conversion. The chiral peptide nucleic acid with *N*-aminoethyl-D proline backbone (base = T^{Bz}) has previously been obtained in 22% overall yield (6 steps) [47] (**Figure 3.19**) while the present method gave the desired products in 40-89 % overall yield (2 steps) depending on the types of nucleobase (**Table 3.1**).

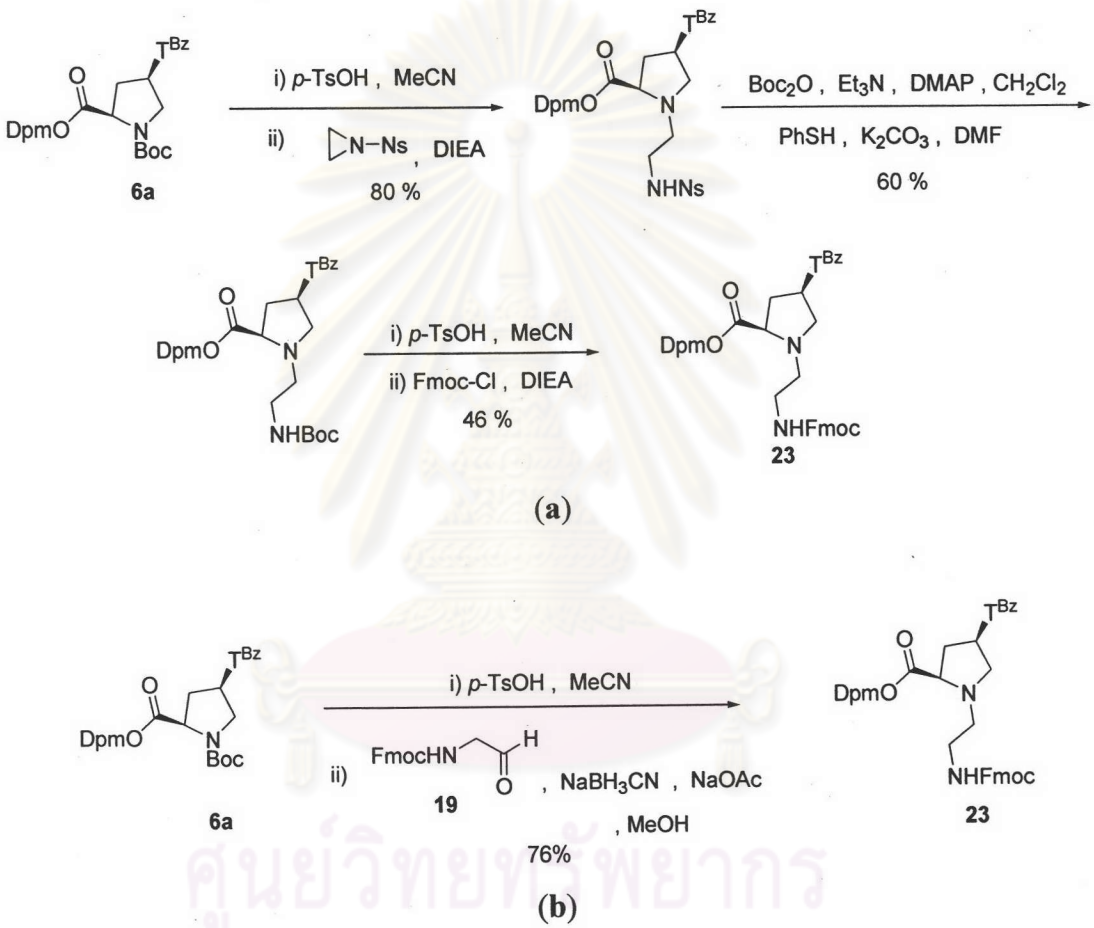

Figure 3.19 Comparison of synthesis of *N*-2-(*N*-Fmoc-amino)ethyl-*cis*-4-*(N*^{3}-benzoyl thymin-1-yl)-D-proline diphenylmethyl ester (**23**) between (**a**) previously reported [47] and (**b**) the present work.

Although these Fmoc-protected compounds **23-29** were stored under low temperature (0 °C), they decomposed slowly on storage. It is possible that the Fmoc was deprotected by the tertiary amine functional group in the compounds themselves **(Figure 3.20).**

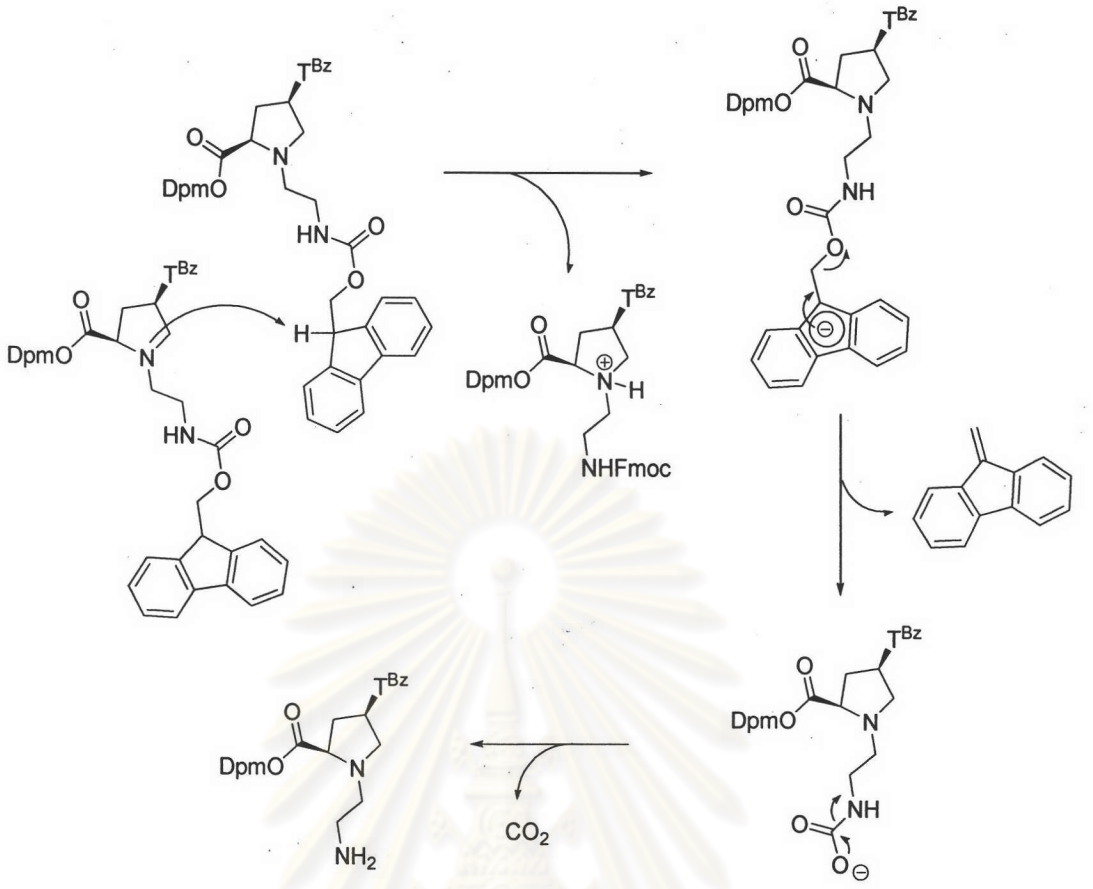

Figure 3.20 Possible mechanism for deprotection of Fmoc protecting group

The next step was selective deprotection of Dpm ester of compound **23-29** in the presence of Fmoc and nucleobase protecting group. Acid condition appeared to be suitable since it has no effect towards the Fmoc protecting group. In case of acid compound, the deprotection of N^3-benzoylthymine compounds (**23-26**) would be the benzoyl group also cleaved. The compounds were treated with trifluoroacetic acid and anisole at ambient temperature overnight to give the desired products. The free acids were easily separated from other by-products washing with diethyl ether to give the TFA salts (**30-36**) as white solid **Table 3.2**.

Table 3.2 Deprotection of Dpm ester

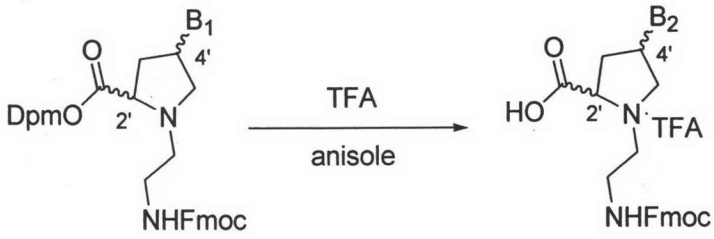

compound	configuration at position 2' and 4'	B_1	product	B_2	% yield
23	(2*R*,4*R*)	T^{Bz}	**30**	T	85
24	(2*S*,4*S*)	T^{Bz}	**31**	T	72
25	(2*R*,4*S*)	T^{Bz}	**32**	T	72
26	(2*S*,4*R*)	T^{Bz}	**33**	T	75
27	(2*R*,4*R*)	G^{Ibu}	**34**	G^{Ibu}	77
28	(2*R*,4*R*)	A^{Bz}	**35**	A^{Bz}	75
29	(2*R*,4*R*)	C^{Bz}	**36**	C^{Bz}	74

From ^{1}H NMR spectra of compounds **30-36** the peaks at 7.00 and 7.24-7.48 ppm of Dpm ester was not observed in all cases indicating complete removal of the Dpm group. In cases of thymine derivatives (**30-33**) the benzoyl peak also disappeared. For example, NMR spectrum of *N*-2-(*N*-Fmoc-amino)ethyl-*cis*-4-T-D-proline (**30**) was compared to *N*-2-(*N*-Fmoc-amino)ethyl-*cis*-4-T^{Bz}-D-proline diphenylmethyl ester (**23**) : C<u>H</u>Ph_2 at 7.00, Dpm aromatic C<u>H</u> at 7.24-7.48, benzoyl C<u>H</u> at 7.51 and benzoyl C<u>H</u> at 7.63-7.77, 7.92-8.00 in ^{1}H NMR spectrum and Dpm aromatic <u>C</u>H at 127.0, 127.2 and 128.8, Dpm aromatic <u>C</u> at 139.4 and 139.5, benzoyl *o*-<u>C</u>H at 129.3, benzoyl *m*-<u>C</u>H at 130.5, benzoyl *p*-<u>C</u>H at 131.7 and benzoyl <u>C</u> at 135.2 in ^{13}C NMR spectrum. It is therefore concluded that the N^3-benzoyl group of thymine was also removed by TFA/anisole. This has previously been observed [54] and should not have subsequent effects on the peptide coupling since the N^3-benzoyl group was not required for the peptide synthesis but was required for the synthesis of the intermediate *via* Mitsunobu reaction. The structure was further confirmed by MALDI-TOF MS analysis (**Table 3.3**).

Table 3.3 Mass spectral data of **30-36** compounds

compound	$M{\cdot}H^+$ (cald)	$M{\cdot}H^+$ (found)
30	505.21	505.13
31	505.21	505.24
32	505.21	505.12
33	505.21	505.00
34	600.26	600.19
35	618.25	618.19
36	594.24	594.11

Condensation reaction between a carboxylic acid and an amine to form amide bond requires activation of the carboxyl group. Although several activation methods are available, Pfp ester was selected as the method of choice due to the ease of synthesis, relative stability and good reactively of the product due to the electron withdrawing effect of the Pfp group.

The free acids were reacted with PfpOTfa and DIEA [54]. This reaction was complete within 1 hr according to TLC analysis. The product was purified by acid-base extraction followed by chromatographic purification. The chromatography must be performed quickly to avoid decomposition of the product on the column. The products were obtained as white foam (**Table 3.4**).

Table 3.4 Protection of Pfp ester

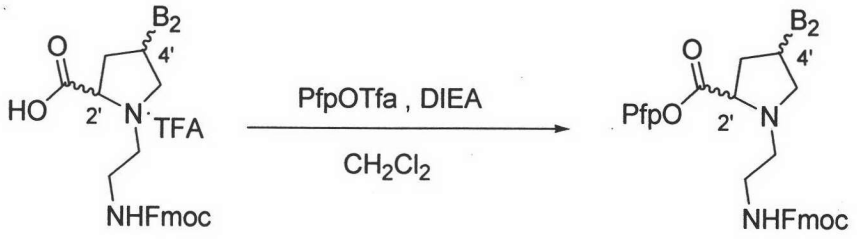

free acid derivative	configuration at position 2' and 4'	B_2	Pfp ester derivative	% yield
30	(2*R*,4*R*)	T	**37**	90
31	(2*S*,4*S*)	T	**38**	89
32	(2*R*,4*S*)	T	**39**	84
33	(2*S*,4*R*)	T	**40**	83
34	(2*R*,4*R*)	G^{Ibu}	**41**	61
35	(2*R*,4*R*)	A^{Bz}	**42**	73
36	(2*R*,4*R*)	C^{Bz}	**43**	70

^{1}H NMR spectra of the free acids derivative and Pfp esters were quite similar. The major difference between polarity of the free acid and Pfp ester derivative were easily identified by TLC. Pfp ester derivative of **37** has R_f = 0.24 (100% ethyl acetate). However, free acid derivative R_f = 0 (100% ethyl acetate). In case of ^{13}C NMR spectra of Pfp esters, the some peak of Pfp ester was similar the free acids and another Pfp ester peak showed a characteristic of Pfp CF such as Fmoc-aminoethyl-*cis*-4-T-D-proline pentafluorophenyl ester (**37**) showed a characteristic pack of Pfp CF at 136.7, 138.5, 139.2,139.7 and 142.2.

The structures of these Pfp esters were further confirmed by MALDI-TOF MS analysis (**Table 3.5**).

Table 3.5 Mass spectral data of **37-43** compounds

compound	MW·H$^+$ (calcd)	MW·H$^+$ (found)
37	671.20	670.96
38	671.20	671.07
39	671.20	671.14
40	671.20	671.14
41	765.23	*
42	784.23	784.37
43	760.22	760.15

*unstable compound

The mechanism for this step was demonstrated in **Figure 3.21.**

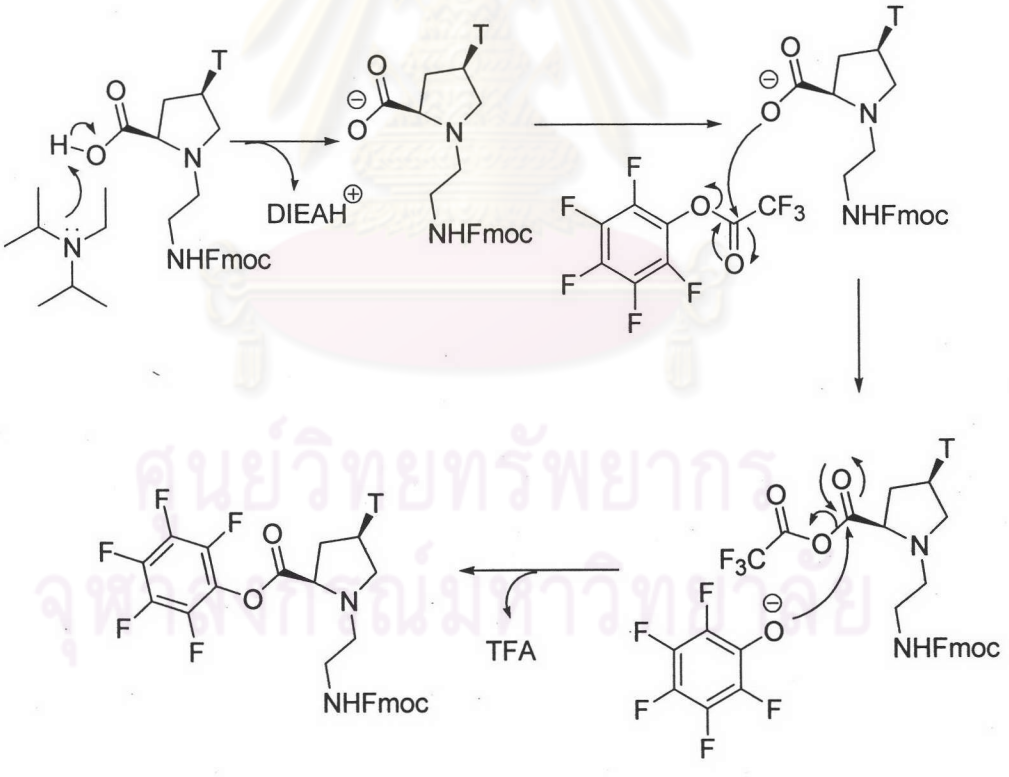

Figure 3.21 Reaction mechanism for synthesis of *N*-2-(*N*-Fmoc-amino)ethyl-*cis*-4-(thymin-1-yl)-D-proline pentafluorophenyl ester (**37**)

The Pfp ester derivatives (**37-43**) were used as monomer in oligomerization which will be described in the next section.

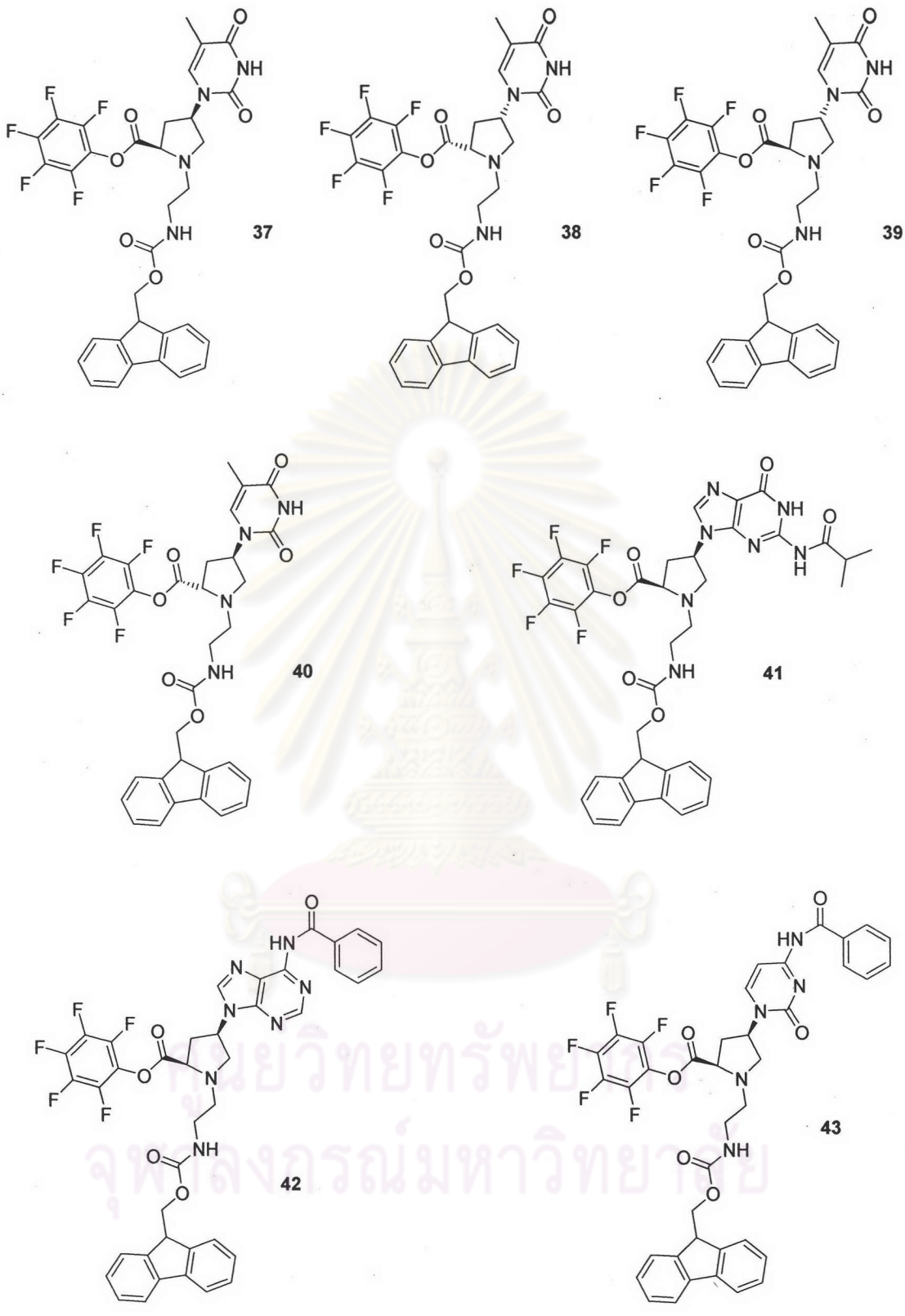

Figure 3.22 Structure of Pfp ester derivatives monomer (**37-43**) for oligomerization

3.2 Oilgomerization of *aep*PNA

Solid Phase Peptide Synthesis (SPPS) was introduced by Merrifield in 1963 [55]. The technique involves growing of a peptide chain from amino acid building blocks on a heterogeneous solid support such as polystyrene resin. The entire process occurs in the same reaction vessel. The reaction involves simple washing and filtration steps therefore minimizing product losses, producing higher-yield (milligram levels of material) and higher-purity peptides.

Synthetic peptides are usually produced in a stepwise fashion starting from C (carboxyl) terminus to N (amino) terminus in a series of coupling cycles. Oligomerization of *aep*PNA monomer was performed by solid phase peptide synthesis methodology as shown in **Table 3.4** The results will be presented and discussed in each part as follows.

Table 3.6 Sequences of decamer *aep*PNA synthesized

structure of decamer *aep*PNA	***ape*PNA monomer.**	**number of monomers required**
CD-Ac-T_{10}-LysNH_2 (**44**)	**37**	10
CL-Ac-T_{10}-LysNH_2 (**45**)	**38**	10
TD-Ac-T_{10}-LysNH_2 (**46**)	**39**	10
TL-Ac-T_{10}-LysNH_2 (**47**)	**40**	10
CD-Ac-A_{10}-LysNH_2 (**48**)	**42**	10
CD-Ac-GTAGATCACT-LysNH_2 (**49**)	**37** **41** **42** **43**	3 2 3 2

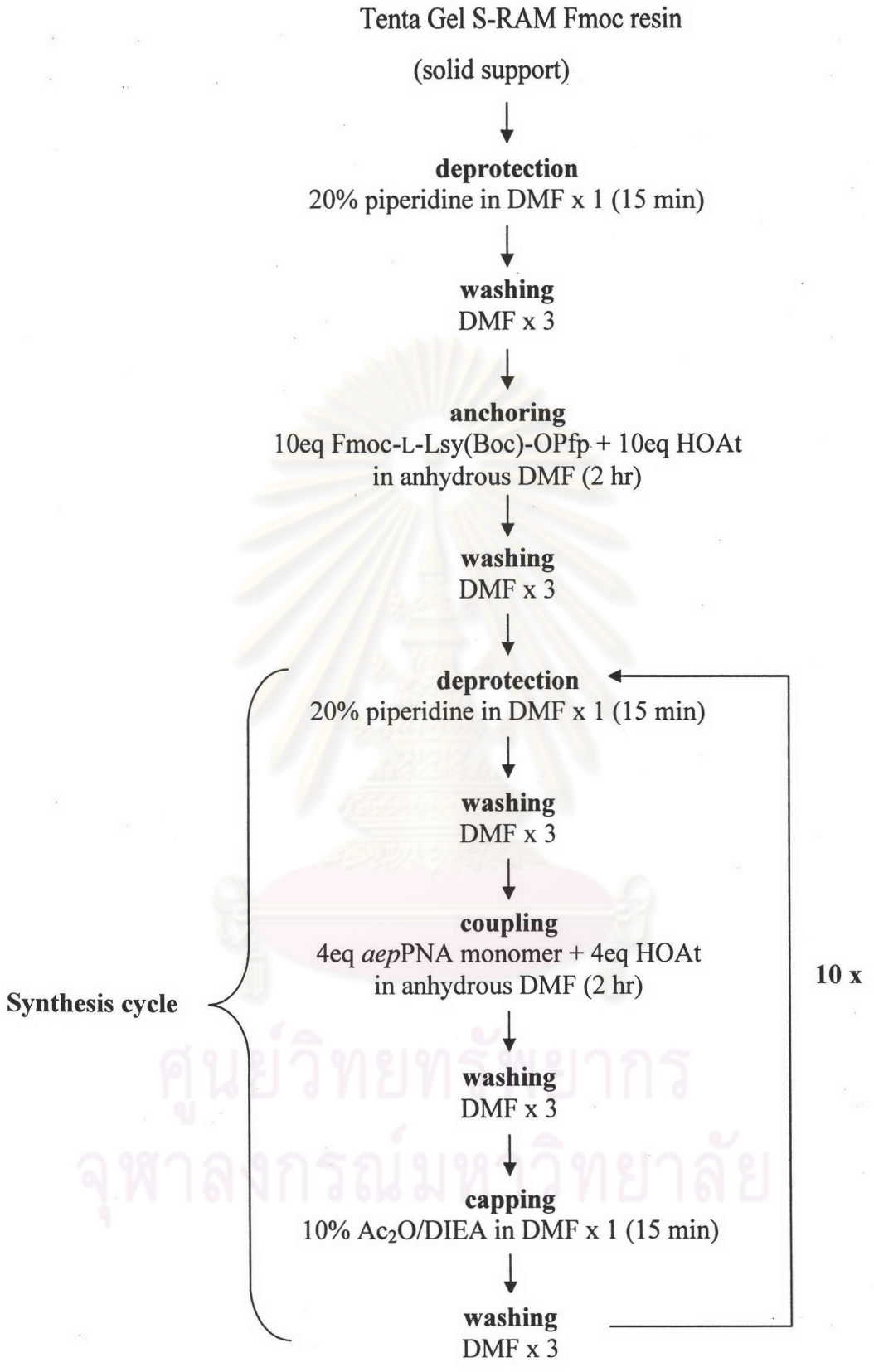

Figure 3.23 The protocol for solid phase synthesis of decamer *aep*PNA [52]

In practice, the manual microscale synthesis of six *aep*PNA (**Table 3.6**) was carried out in pipette as described in section 2.2.1 using the standard protected described by Vilaivan for synthesis of this and other similar PNA [54] (**Figure 3.23**). RAM resin (**Figure 3.24**) is more acid labile than MBHA resin and Wang resin, the peptide-linker bonds are easily cleaved with 60-95 % TFA to provide peptide amides. In addition, RAM resin is also stable to piperidine, it is therefore compatible to Fmoc chemisty for solid phase. Moreover, the amino linker of RAM resin allow easy coupling with active esters to form amide bonds therefore giving higher loading efficiency compared to resins containing hydroxyl linker such as Wang resin.

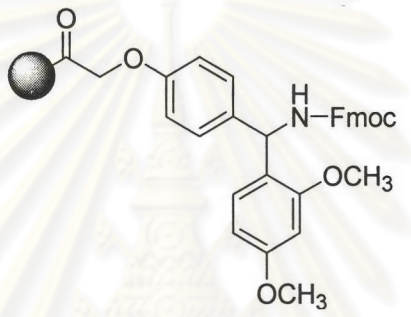

Figure 3.24 TentaGel S RAM Fmoc resin

The Tenta Gel S-RAM Fmoc resin contains PEG modifier which is swellable in many solvents, making it an ideal support for peptide synthesis. First of all, the resin was swollen in anhydrous DMF. In the next step, the deprotection was carried out by treatment of the resin with 20% piperidine in DMF for 15 min in order to remove the terminal Fmoc protecting group which was released from the resin-bond peptide as the piperidine-dibenzofulvene adduct by E_1CB-type mechanism type of E1cb via the stabilized dibenzocyclopentadienyl anion as shown in **Figure 3.25**

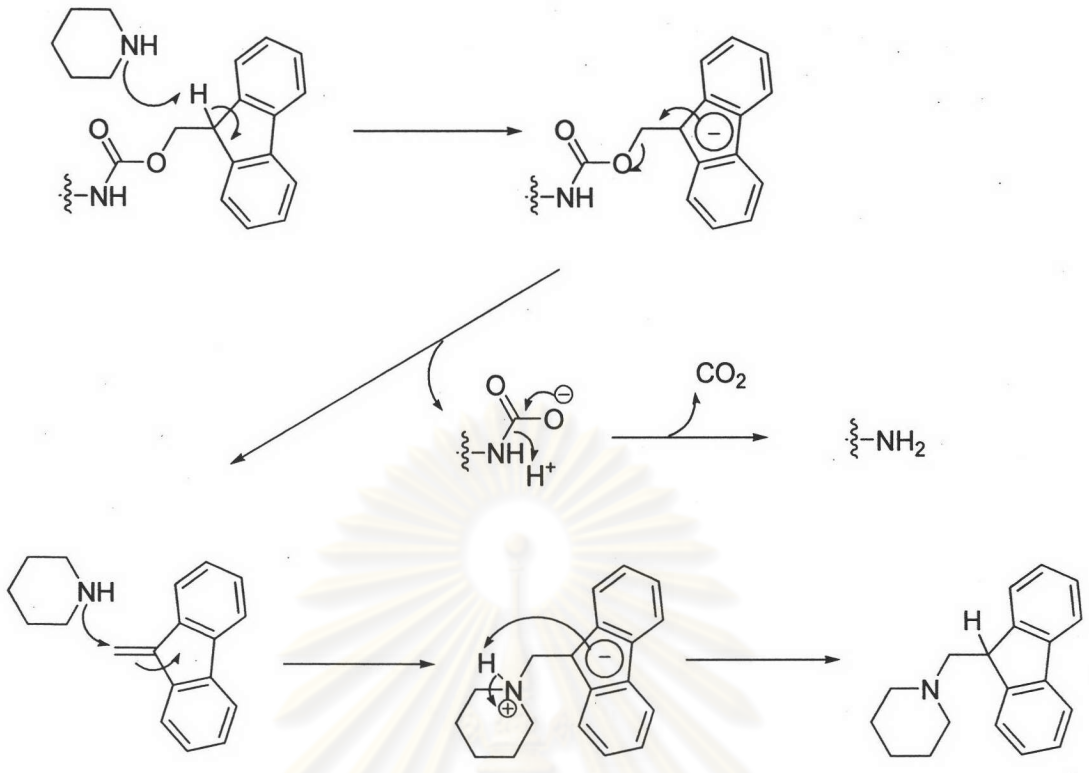

Figure 3.25 Mechanism for deprotection of Fmoc protecting group from resin bound peptide

It has also been suggested that introducing a lysine at C-terminus of peptide chain could serve to prevent the self aggregation of the peptide chain due to the repulsion of the positively charged side chain and also increased the solubility of the peptide in aqueous medium [3,4,5,7]. After deprotection, the resin was anchored with Fmoc-Lys(Boc)-OPfp as the first amino acid residue in the presence of HOAt as an auxiliary nucleophile or "activater" according to the mechanism in **Figure 3.26**. Due to its heterogeneous nature of SPPS, the reaction would not be completed simply with 1:1 stoichiometric proportion of reactant and would require a very long reaction time. Bearing this in mind, excess and high concentration (2-10 equivalent) of coupling reagents were generally used in order to enhance the coupling efficiency within a reasonable time scale.

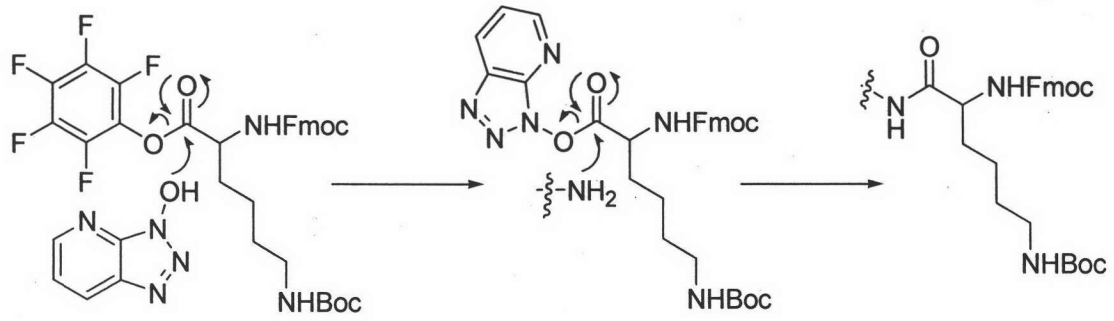

Figure 3.26 The mechanism for coupling of anchoring *via* HOAt activation

The next step of the synthesis cycle consisted of deprotection of the Fmoc group, coupling with a monomer and capping, extensive washing with DMF was performed after each step.

Estimation of the coupling efficiency could be performed by diluting the resulting deprotecting solution with an appropriate volume of absolute methanol and then the UV-absorption of the piperidine-dibenzofulvene adduct measured at 264 nm. This number is related to the total amounts of Fmoc group remained on the resin-bond peptide before deprotection step and indirectly indicated the efficiency of previous coupling cycle. For convenience, it was proposed that the first absorption value of which obtained after deprotection of Fmoc-Lys-peptide-resin corresponded to 100 % coupling efficiency. Therefore comparison of the net absorption with this initial value could be used to calculate the percent of coupling efficiency after each coupling step and the overall efficiency of the synthesis could be evaluated. In practice even after coupling with excess reagent, the coupling efficiency was not always approaching 100%. Some of the residual free amino groups on the resin have not been coupled and was still reactive enough to react with the monomer in the next coupling cycle. This situation was therefore resulted in skipping of one coupling cycle which brought about missing of a repeating unit in peptide chain. In fact, this might happen more than once and might occur anywhere in peptide chain. The resulting "incomplete peptide" is generally called "deletion sequences" and would contaminate the peptide product. Worse still, those truncated peptide generally possess similar polarity to the desired peptides product which led to difficulty in purification. However it was possible to solve this problem by acetylation the unreacted amino group residue at N-terminus on resin bond peptide into acetamide derivative with 10% acetic

anhydride/DIEA in DMF in order to change the polarity of truncated peptide chain and also to diminish the nucleophilicity of the nitrogen atom at N-terminus as an acetamide which would not be able to grow in the next coupling cycles. This acetylation procedure is normally called "capping" and is sometime considered as optional for solid phase synthesis. However, we decided to perform this ended capping every time after coupling step was finished for easier purification. The synthesis cycle was repeated until the growing peptide chain was extended up to decamer. After final cleavage of Fmoc, the *N*-terminus was to prevent intramolecular cyclization initiated by the free amino group at the *N*-terminus.

In cases of decamer *aep*PNA **48** and **49**, the nucleobase protecting groups (Bz, Ibu) remains on the peptide chain. This must be first deprotected after completion of the synthesis by treatment of the resin with aqueous ammonia/dioxane 1:1 at 60 °C for 6 h. Finally, the total peptide was released from the resin by treatment with trifluoroacetic acid for 3 h during which time the resin became gradually red. The volatile trifluoroacetic acid was removed by a gentle stream of nitrogen which gave sticky residue which after treatment with diethyl ether yielded a white precipitate which washed with ether and air dried.

The crude peptide was dissolved in water and the concentration determined calculated from UV-absorption and the coupling efficiency in each decamer was calculated to be percentage as shown in **Table 3.7**.

Table 3.7 The UV-absorption data and percent coupling efficiency of all decamer *aep*PNA

decamer ***aep*PNA**	**scale (μmol)**	**%efficiency*** **(overall)**	**OD_{264} (water 200 μL)**
CD-Ac-T_{10}-LysNH_2 (**44**)	1.5	66	363
CL-Ac-T_{10}-LysNH_2 (**45**)	1.5	80	378
TD-Ac-T_{10}-LysNH_2 (**46**)	1.5	72	398
TL-Ac-T_{10}-LysNH_2 (**47**)	1.0	74	295
CD-Ac-A_{10}-LysNH_2 (**48**)	1.5	67	552
CD-Ac-GTAGATCACT-Lys NH_2 (**49**)	0.5	81	108

*calculated by absorbance of deprotection of Fmoc lysine with deprotection of last monomer.

The crude peptide was purified by reverse phase HPLC using the gradient system as described in section **2.2.3 (b)**, **(c)** and **(d)**. The example chromatograms of CD-Ac-T_{10}-Lys NH_2 (**44**) were shown in **figure 3.27**

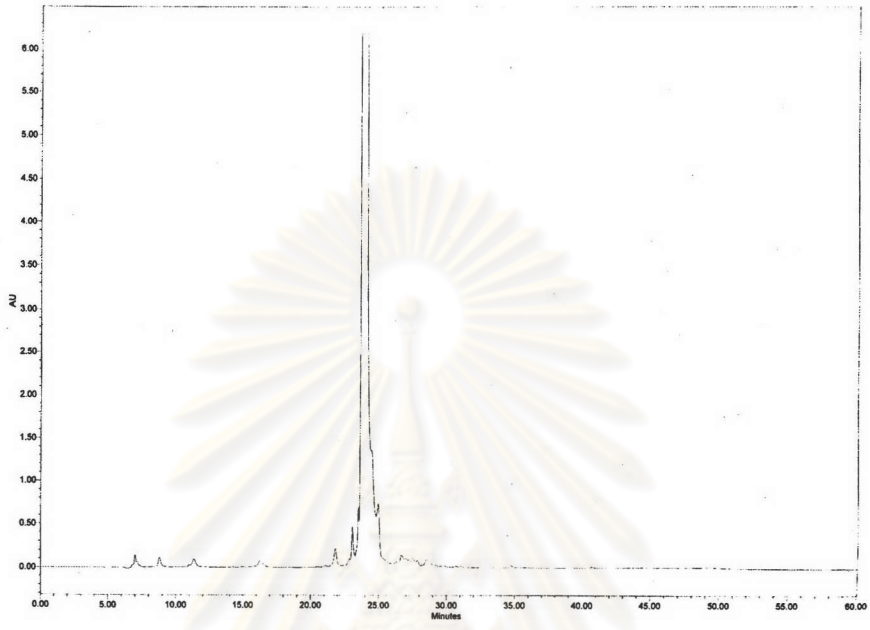

(a)

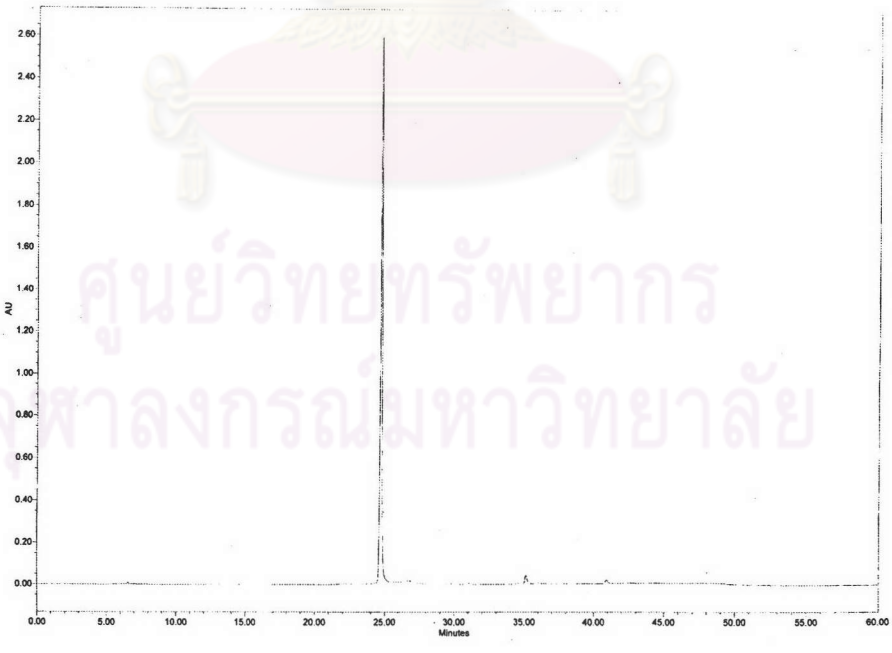

(b)

Figure 3.27 Chromatograms of CD-Ac-T_{10}-LysNH_2 (**44**) (**a**) before and (**b**) after purified by reverse phase HPLC

The decamer *aep*PNAs were obtained after reverse phase HPLC separation as a single sharp peak **(Figure 3.27)** and were characterized by MALDI-TOF mass spectrometry **(Table 3.8)**

Table 3.8 Mass spectral data of all decamer *aep*PNA

decamer *aep*PNA	**$M{\cdot}H^+$ (calcd)**	**$M{\cdot}H^+$ (found)**
CD-Ac-T_{10}-LysNH_2 (**44**)	2830.05	2830.04
CL-Ac-T_{10}-LysNH_2 (**45**)	2830.05	2830.27
TD-Ac-T_{10}-LysNH_2 (**46**)	2830.05	2830.24
TL-Ac-T_{10}-LysNH_2 (**47**)	2830.05	2830.31
CD-Ac-A_{10}-LysNH_2 (**48**)	2920.18	2920.03
CD-Ac-GTAGATCACT-LysNH_2 (**49**)	2877.09	2877.57

In all cases the quasi-molecular ions were clearly observed with MW within ±0.5 Da to the calculated values, thus confirming the identities of all PNA synthesized.

3.3 Biophysical studies

DNA denaturation refers to the melting of double stranded DNA to generate two single strands. This involves the breaking of hydrogen bonds between the bases in the duplex. The purine and pyrimidine bases in DNA absorb UV light maximally at a wavelength of approximately 260 nm (**Figure 3.28**) [56]. In double-stranded DNA, however, the absorption is decreased due to base-stacking interactions. When DNA is denatured, these interactions are disrupted and an increase in absorbance is seen. This change is called the hyperchromic effect. The extent of the effect can be monitored as a function of temperature. The denaturation of double stranded DNA is therefore easily followed spectrophotometrically.

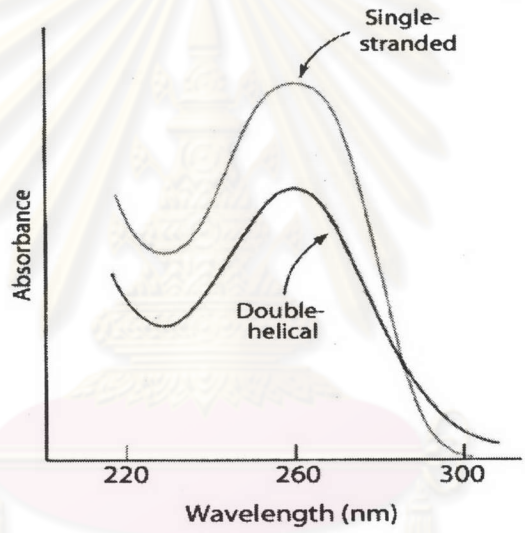

Figure 3.28 The UV absorbance of single stranded DNA and double helical DNA.

Measurement of the absorbance of a DNA complex at 260 nm while slowly increasing the temperature provides a means to observe denaturation. In a thermal denaturation experiment monitored using absorption spectroscopy, the polynucleotide absorbance typically changes very slowly at first, then rapidly rises to a maximum value (**Figure 3.29**). The temperature at which the DNA molecules are 50 % denatured is the melting temperature (T_m)

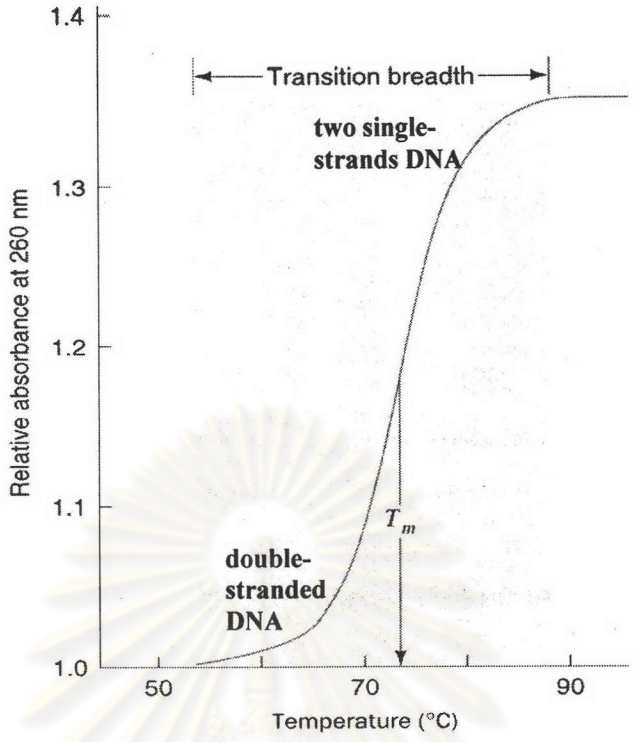

Figure 3.29 The UV absorbance of T_m experiment

Interaction between the decamer *aep*PNA with poly(rA), poly(dA), poly(rU) and poly(dT) was investigated by T_m measurement. Due to availability and cost, we chose dA_{50} and dT_{50} as models of poly(dA) and poly(dT) respectively. The thermal transition curves of the above decamers were recorded at 260 nm over 20-90 °C range (**Figure 3.30-3.32**) and T_m values are as shown in **Table 3.9.**

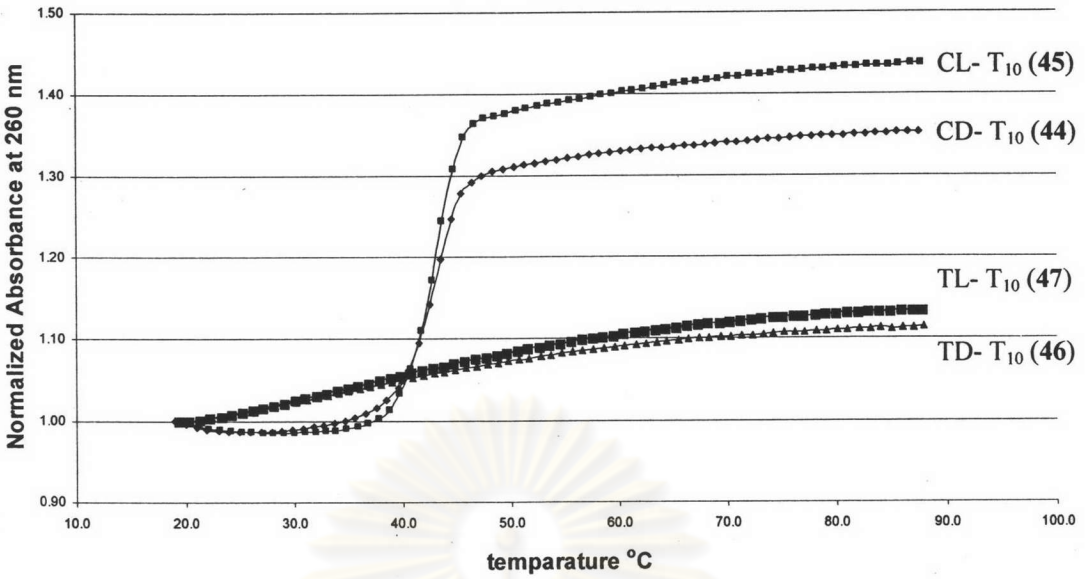

Figure 3.30 Melting curves of **44**, **45**, **46** and **47** with poly(rA). Condition: 10 mM sodium phosphate buffer pH 7.0 1.0 μM decamer (**44**, **45**, **46** and **47**), ratio of T:A = 1:1

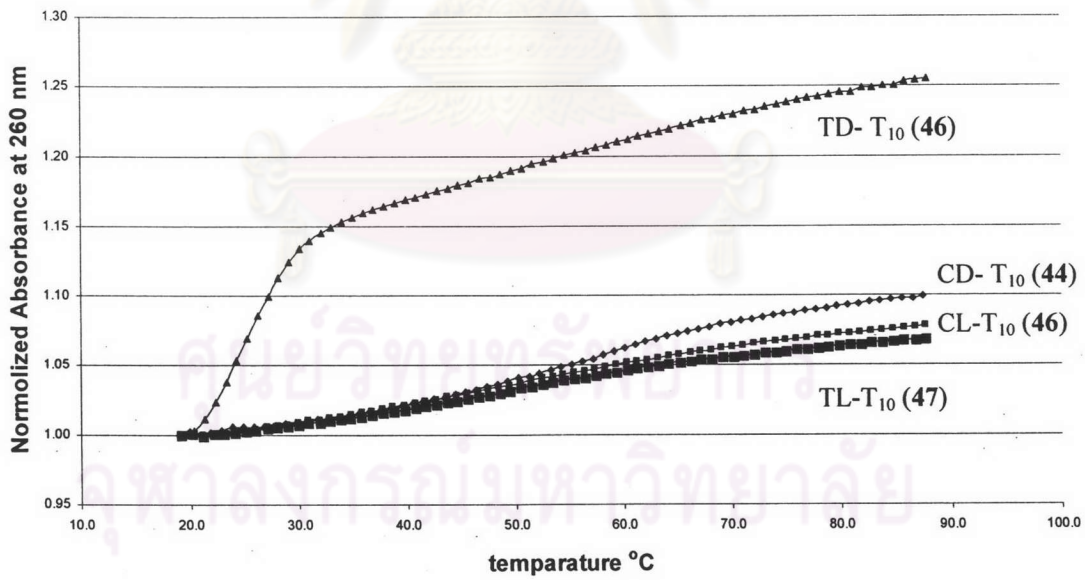

Figure 3.31 Melting curves of **44**, **45**, **46** and **47** with dA_{50}. Condition: 10 mM sodium phosphate buffer pH 7.0 1.0 μM decamer (**44**, **45**, **46** and **47**), ratio of T:A = 1:1

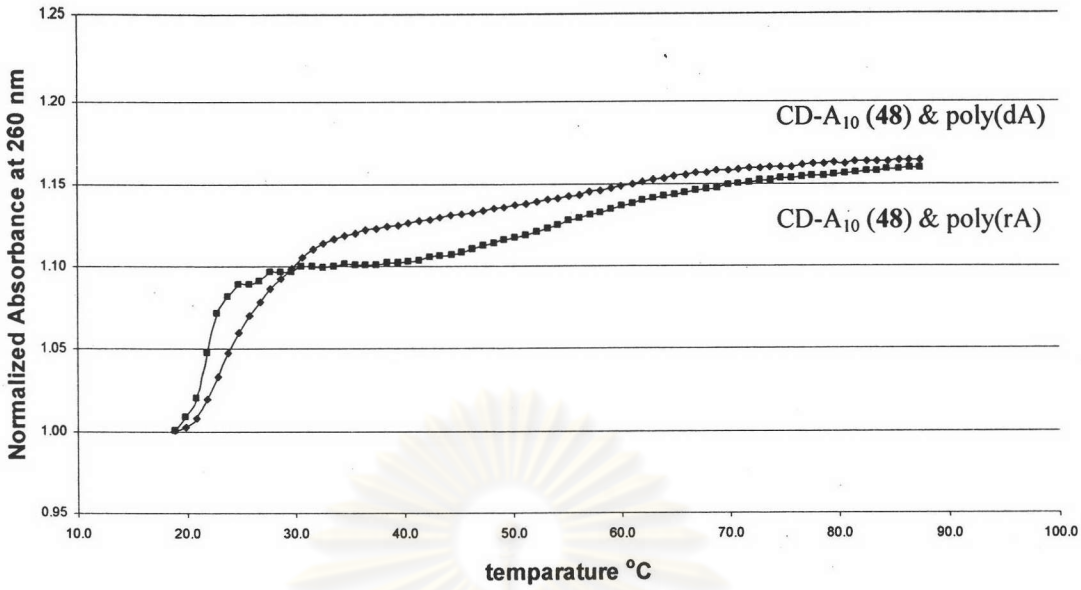

Figure 3.32 Melting curves of **44** with poly(rA) and dA_{50}, **48** with poly(rU) and dT_{50}. Condition: 10 mM sodium phosphate buffer pH 7.0 1.0 μM decamer (**44** and **48**), ratio of T:A = 1:1 and U:A = 1:1

Table 3.9 T_m values of hybrids between decamer *aep*PNA and polynucleotides

decamer *aep*PNA	polynucleotide	T_m
CD-Ac-T_{10}-LysNH_2 (**44**)	poly(rA)	42
CL-Ac-T_{10}-LysNH_2 (**45**)	poly(rA)	43
TD-Ac-T_{10}-LysNH_2 (**46**)	poly(rA)	n.d.
TL-Ac-T_{10}-LysNH_2 (**47**)	poly(rA)	n.d.
CD-Ac-T_{10}-LysNH_2 (**44**)	dA_{50}	n.d.
TD-Ac-T_{10}-LysNH_2 (**45**)	dA_{50}	24
CL-Ac-T_{10}-LysNH_2 (**46**)	dA_{50}	n.d.
TL-Ac-T_{10}-LysNH_2 (**47**)	dA_{50}	n.d.
CD-Ac-A_{10}-LysNH_2 (**48**)	poly(rU)	21
CD-Ac-A_{10}-LysNH_2 (**48**)	dT_{50}	23

n.d. : not detectable

The binding experiments clearly indicate that the CD-Ac-T_{10}-LysNH_2 (**44**) and CL-Ac-T_{10}-LysNH_2 (**45**) formed stable hybrids with poly(rA) (T_m 42 and 43 °C) but they could not form hybrids with poly(dA). On the other hand, TD-Ac-T_{10}-LysNH_2

(**46**) failed to form stable hybrid with poly(rA) but it forms a rather unstable PNA·DNA hybrid with a T_m of 24 °C. TL-Ac-T_{10}-LysNH_2 (**47**) neither bound to DNA nor RNA, whereas CD-Ac-A_{10}-LysNH_2 (**48**) bound both DNA and RNA with similar affinities: T_m 21 and 23 °C respectively. Therefore both base sequences and the stereochemistries on the pyrolidine ring can have a dramatic effect on the binding characteristics of the *aep*PNA.

The hybridization property of the thymine oligomer CL-*aep*PNA has been previously reported by Kumar and Lui. According to the reslts of Kumar [44], T_m of CL-*aep*PNA T_8: dA_8 complex was proposed to be too high to be measured (>80 °C). On the other hand, Lui has reported that the CL-*aep*PNA T_{10} did not bind with its complementary DNA target [46]. In this research, CL-Ac-T_{10}-LysNH_2 (**45**) could not hybridize with poly(dA), thus confirming Lui's results.

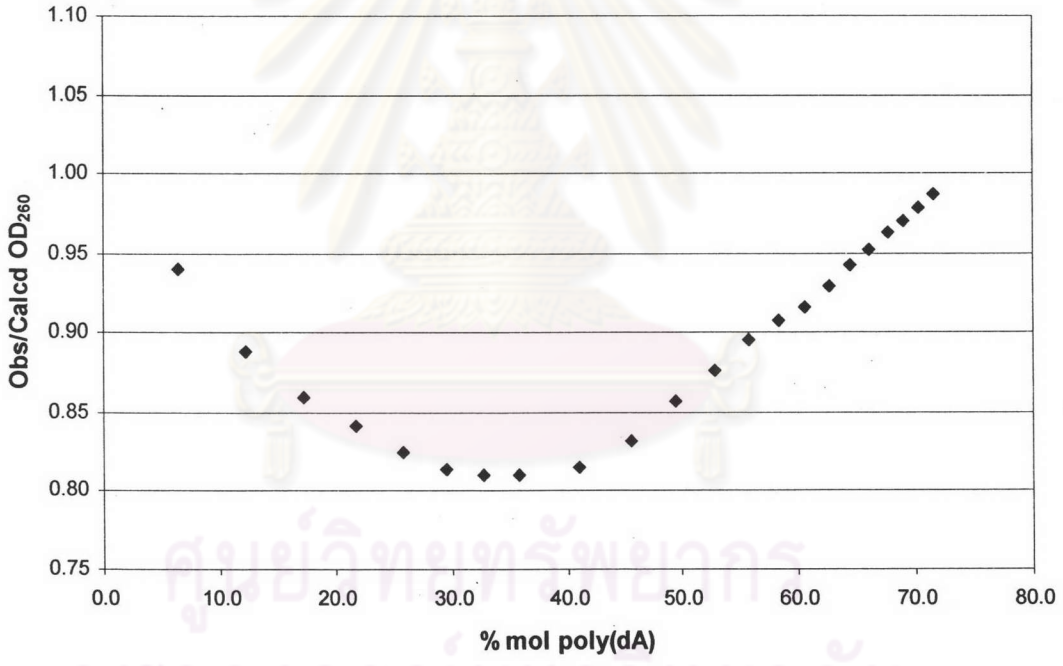

Figure 3.33 UV titration of CD-Ac-T_{10}-LysNH_2 (**44**) and poly(rA). The concentration of CD-Ac-T_{10}-LysNH_2 (**44**) being kept constant at 2.39 μM. The solution was buffered with 10 mM sodium phosphate.

The UV titration between CD-Ac-T_{10}-LysNH_2 (**44**) and poly(rA) (**Figure 3.33**) revealed a 2:1 stoichiometry of T:A, indicating the formation of a triple helical complex, probably *via* Watson-Crick and Hoogsteen-type T·A·T pairing similar to that reported by Vilaivan *et al.* [47].

It should be noted that the results mentioned above must be regarded as a preliminary study only. In order to gain more complete pictures further investigation of *aep*PNA is still required.